

CNIC-01104

GIEC-0002



CN9700766

中国核科技报告

CHINA NUCLEAR SCIENCE AND TECHNOLOGY REPORT

江西省地热背景与地下热水同位素地球化学研究

STUDIES OF GEOTHERMAL BACKGROUND
AND ISOTOPIC GEOCHEMISTRY OF
THERMAL WATER IN JIANGXI PROVINCE



中国核情报中心
原子能出版社

China Nuclear Information Centre
Atomic Energy Press



周文斌：副教授，华东地质学院副院长。1982年
毕业于华东地质学院地质系水文地质与工程地
质专业。

ZHOU Wenbin: Associate professor, deputy
president of East China Geological Institute.
Graduated from Geological Department of East
China Geological Institute in 1982, majoring in
hydrogeology and engineering geology.

CNIC-001104

GIEC-0002

江西省地热背景与地下热水 同位素地球化学研究

周文斌 孙占学 李学礼 史维浚

(华东地质学院, 江西临川)

摘 要

在江西省进行了大地热流测量, 并对江西境内的水热系统进行了系统的同位素和地球化学研究。结果表明江西地下热水属于中、低温对流型地热系统, 它们与深部有岩浆热源的高温地热系统有明显区别。同时证明同位素和地球化学技术对地热资源勘查十分有效。

Studies of Geothermal Background and Isotopic Geochemistry of Thermal Waters in Jiangxi Province

ZHOU Wenbin SUN Zhanxue LI Xueli SHI Weijun

(East China Geological Institute, Linchuan, Jiangxi)

ABSTRACT

The terrestrial heat flow measurement, isotope and geochemical techniques have been systematically applied to the geothermal systems in Jiangxi Province. Results show that the thermal waters in the study area all belong to the low-medium temperature convective geothermal system, which essentially differs from high temperature geothermal systems with deep magmatic heat sources. It has been proven that the isotope and geochemical techniques are very useful and effective in geothermal exploration.

INTRODUCTION

Thermal waters are widely distributed in Jiangxi Province and their genesis and origin have been a subject of dispute for a long time. In 1989, we were supported by the China National Fund of Natural Sciences to carry out a project to approach the geothermal background of Jiangxi Province and its relations with hydrothermal uranium mineralization. In 1991, the International Atomic Energy Agency (IAEA) decided to fund the project of research contract entitled " An Oxygen and Hydrogen Isotope Study of Thermal Springs in Jiangxi Province" as a part of the " Regional Coordinated Project on Isotope and Geochemistry in Geothermal Exploration Areas in Africa, Asia and the Pacific and the Middle East". According to the Research Contract (No. 6447/R0/RB and No. 6447/R1/RB) signed between the IAEA and the East China Geological Institute, the programme of the work included: (1) Monitoring of hot springs and ground water in Jiangxi Province for isotopic and geo chemical analyses; (2) Elaboration of the data to evaluate the formation conditions of hot springs. This paper will demonstrate the major results of the above-mentioned programs.

1 GEOLOGICAL SETTING

Jiangxi Province is located in the southeastern coastal area of China. Roughly divided by the Zhe-Gan Railway, Jiangxi lies on two major tectonic units, the north belonging to the southeastern margin of Yangtze Metaplatform, and the center and south being a part of the southern China Fold System.

Jiangxi Province has a multilayered and heterogeneous deep structures, and the tectonic landforms has a mirror symmetry with the fluctuation of the Moho. The deep structure can be divided into three types (see Fig. 1), in which (1) the lifted zone of the upper mantle, (2) the sunken zone of the upper mantle, and (3) the transitional zone of the deep structure.

Faults are well developed in Jiangxi and can be classified into four groups: the nearly E W group (mainly in the Yangtze Metaplatform), the NE-NEE group (mainly in the center and south), the NNE-nearly SN group (mainly in the center and south) and the NW group (mainly in the center-south and the north east) in which the nearly NE-NNE group was mostly developed and followed by the nearly EW-nearly SN group. It had been proved that there are 10 pieces of deep faults and 8 pieces of great faults in Jiangxi Province (Fig. 1). The deep faults began to devel-

op in the later stage of the basement folding and fell into the present pattern in the Indo-Chinese epoch and Yanshan epoch. Expanded and deepened in multiple movement, these faults controlled the volcanic and igneous activities, the formation of red basins, diageneses, mineralizations, hot spring distribution and regional geothermal regime.

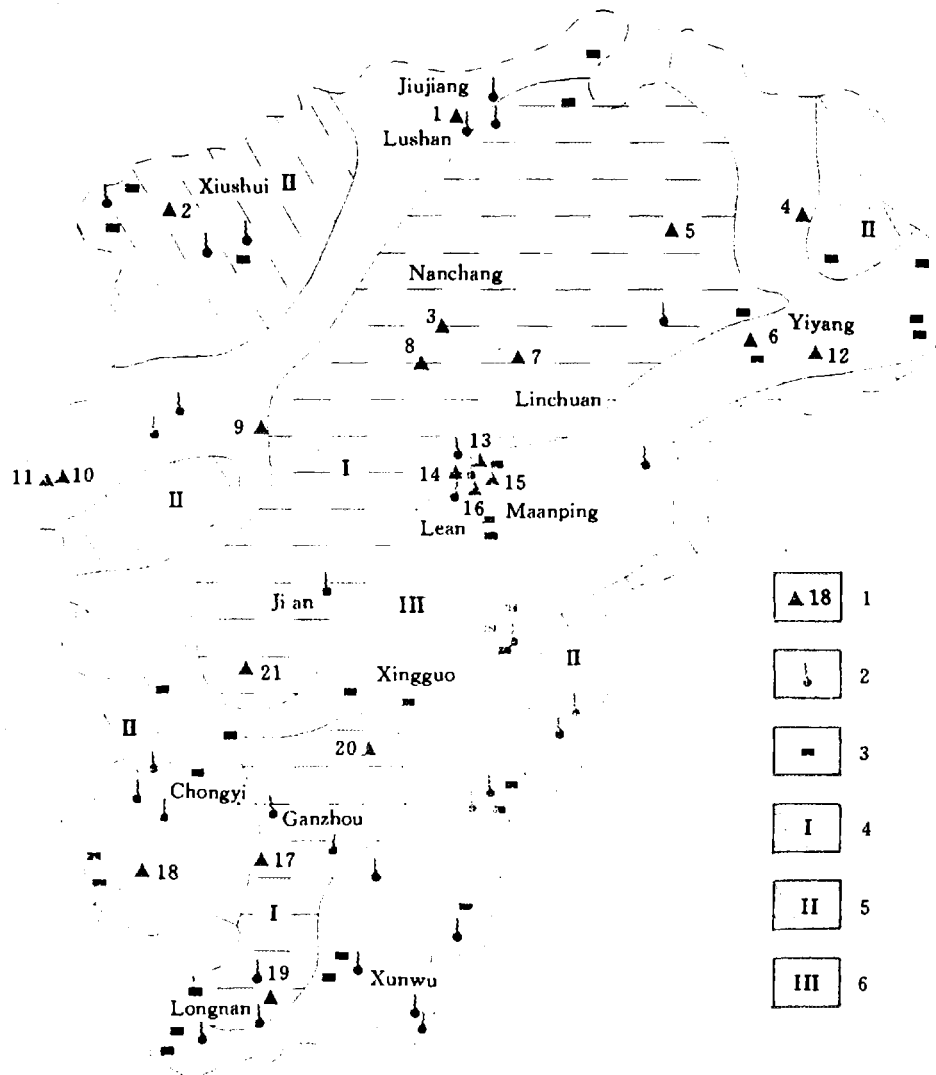


Fig. 1 Schematic map showing the tectonic units, heat flow points, hot springs and uranium mineralization distribution

1. heat flow measurement points; 2. hot springs; 3. U mineralization points;
4. lifted area of the upper mantle; 5. sunken area of the upper mantle; 6. structural transitional zone.

2 GEOTHERMAL BACKGROUND

2.1 Terrestrial heat flow

Terrestrial heat flow is key to learn the geothermal regime of the concerned area. By definition, terrestrial heat flow is given as follows:

$$q = K \frac{dT}{dZ} \quad (1)$$

where, q —terrestrial heat flow, mW/m^2 ; K —heat conductivity of media, $\text{W}/\text{m}^\circ\text{C}$; T —temperature, $^\circ\text{C}$; Z —depth, m , $\frac{dT}{dZ}$ —geothermal gradient $^\circ\text{C}/\text{km}$.

From 1987 through 1990, East China Geological Institute, co-operated with Institute of Geology, Academia Sinica, measured 16 terrestrial heat flow values for Jiangxi province for the first time. Temperature measurement has been made for 26 bore-holes with depth from 110 to 1040 m, and 172 pieces of rock samples have been collected to determine their heat conductivities.

According to Table 1, the terrestrial heat flow values for Jiangxi Province vary from 57.8 to 82.1 mW/m^2 , averaging 70.5 mW/m^2 , accord with the regional heat flow for the southeastern coastal area of China. Fig. 1 also shows the heat flow anomalies in Jiangxi, such as Dexing and Rongnan. In summary, the anomalies have the following characteristics:

(1) Along the transitional zone of deep structure, that is, the positions between the lifted zone and sunken zone of upper mantle where great changes take place, the heat flows increase apparently (or anomalies);

(2) The heat flows become considerably higher (or anomal) along the active deep faults;

(3) The heat flow anomalies are in accordance with presently active hydrothermal activities and Mesozoic-Cenozoic volcanic-igneous activities in distribution.

(4) The heat flows increase greatly in uranium-riched rocks and uranium deposits.

2.2 Affecting Factors

2.2.1 Geological structure

Researches reveal that heat flow values are different in different tectonic units. In old and stable platform areas, heat flow values are lower and more homogenous than those in young orogenic belts and rift zones. Generally speaking, the younger the tectonic units and the stronger activities of structures are, the higher the heat flow values. The distribution of heat flow in Jiangxi province reflects such laws. Owing to that northern Jiangxi belongs to Yangtze Metaplatform which is a stable massif while central and southern Jiangxi is a part of South China Fold System which is an active land mass, heat flow values in the former are lower than those in the latter.

Table 1 Data of measured and corrected heat flow values in Jiangxi Province

No.	Loaction	Longitude	Latitude	Depth m	Rock	Gradient $\frac{G \pm SD}{C/km}$	Conductivity $\frac{K \pm SD}{W/(mC)}$	Heat flow	
								Measured	Corrected mW/m^2
1	Ruichang	115°38'	29°40'	390~500	sandstone	19.27±1.05	3.07±0.07	59.2	
2	Nanchang	115°52'	28°23'	230~750	mudstone	23.70±0.58	2.38±0.08	56.4	
				750~1040	sandstone	17.98±0.43	3.48±0.16	62.5	58.6 ^{a)}
3	Xiushui	114°22'	29°01'	40~260	mudstone	21.00±1.12	2.75±0.01	57.8	
4	Dexing	117°41'	28°55'	760~940	phyllite	20.94±0.67	4.40±1.18	92.1	72.2 ^{b)}
5	Leping	117°01'	28°55'	645~765	sandstone	25.00±0.00	3.30±0.44	82.5	
6	Yiyang	117°26'	28°21'	220~310	tufistone	27.40±1.00	2.90±0.11	79.5	
7	Jinxian	116°13'	28°16'	90~170	meta-sandstone	23.15±2.84	3.04±0.21	70.4	
8	Fengcheng	115°49'	28°15'	140~280	sand-mudstone	20.33±0.66	3.28±0.64	66.7	
				390~470	limestone	21.95±0.92	3.11±0.23	68.2	67.3 ^{a)}
9	Xinyu	114°59'	27°55'	382~502	mud-sandstone	28.67±1.46	2.76±0.07	79.2	
10	Pingxiang	113°48'	27°32'	40~210	sandstone	17.43±0.46	3.85	67.1	
11	Pingxiang	113°48'	27°32'	200~320	tuff, sandstone	22.39±0.70	3.98±1.16	89.1	72.6
12	Yongping	117°43'	28°14'	20~110	migmatite	20.30±2.20	3.26±0.29	66.2	
13	Lean	115°58'	27°45'	100~260	porphyroclastic lava	20.17±0.30	3.25±0.20	65.6	
				280~370	dacite	22.03±1.65	3.23±13	71.2	67.6 ^{a,d)}
14	Lean	115°58'	27°45'	440~940	porphyroclastic lava	32.19±1.40	3.14±0.15	101.0	79.9 ^{b,d)}
15	Lean	115°58'	27°45'	320~430	porphyroclastic lava	25.85±1.70	3.02±	78.0	62.3 ^{d)}
16	Lean	115°58'	27°45'	100~300	porphyroclastic lava	26.84±1.14	3.02±	81.0	74.6 ^{d)}
17	Ganzhou	114°51'	25°45'	100~300	sandstone, shale	33.63±2.26	2.18±0.14	73.3	62.1 ^{c)}
18	Chongyi	114°21'	25°33'	70~260	granite	26.03±0.71	3.34±0.06	86.9	75.6 ^{b)}
19	Longnan	114°46'	24°52'	300~390	sandstone	17.92±1.83	3.75±0.68	67.2	

a, b, c, d) separately stand for average heat flow of different measure section for a bore-hole, heat reflect correction, groundwater disturbance correction and radiogenic heat correction.

It can be seen from Fig. 1 that the distribution of surface heat flow anomalies are controlled by deep seated structural transitional zones and deep-great faults (or fault basins). Heat flow values in the deep-great fault zones (or along fault basins) are markedly high. For examples, heat flow value is high up to 72.2 mW/m² in Yingshan, Dexing county that is in Xichuang-Dexing fault zone. The reason for this kind of distribution could be as follows:

(1) The heat flow contributed by the friction heat from faulting, for instance, the calculated quantity of the heat by Shicheng-Xunwu fault within the depth of

5 km is calculated to be 2.24 mW/m^2 , making up 3.03% of the total surface heat flow (74 mW/m^2). The result of calculation is shown in Table 2;

(2) The deep-great faults serve as the passage, conducting the heat from the deep earth and resulting higher heat flow near by the fault;

(3) The fault surfaces could affect and redistribute the heat flow.

Because faults can not only conduct heat from the depth and produce friction heat, but also cause redistribution and refraction of surface heat flow as physical boundaries, heat flow are influenced by fault structures.

The deep seated structural transitional zone, that is the part where the lifted area turns into the sunk area in the upper mantle, apparently controls the heat flow anomalies. Eight heat flow anomalies found in Jiangxi Province are in or near the transitional zones except Fengcheng. The deep seated structural transitional zone is a special geological structural unit in which tectonic stress is concentrated, and deep geological activities are frequent. Therefore, the distribution of heat flow anomalies are generally influenced by the transitional zones.

Similar to heat flow anomalies, uranium deposits (mainly hydrothermal ones) are partially controlled by deep-great faults and deep seated structural transitional-zones. Deep-great faults controlling of uranium mineralization is well known. Researches of uranium deposits distribution laws show that most uranium deposits, especially the mid-large scale ones distribute mainly in the deep seated structural transitional zones. The evidence reveals that uranium mineralizations are obviously controlled by the transitional zones (Fig. 1)

Distribution of heat flow anomalies is in accordance with that of uranium mineralization because they are both controlled by deep-great faults and deep seated structural transitional zones.

2.2.2 Enrichment of radioactive elements

Radioactive heat is major source of heat energy of the earth interior, and enrichment of radioactive elements, such as uranium, thorium and potassium-40, affect the terrestrial heat flow to different extent. Taking Xiangshan Uranium Ore-field as an example, the following paragraphs will discuss the influence of radioactive elements on heat flow.

Xiangshan Uranium Ore-field consists of dozens of hydrothermal uranium deposits within a Mesozoic volcanic basin in the southeastern China. The terrestrial heat flow tends to increase from 62.3 mW/m^2 at the edge to 83.5 mW/m^2 in the center of the basin. In addition to the influence of deep faults, the radioactive heat

greatly contribute to the distribution of heat flow for Xiangshan Uranium Ore-field.

2. 2. 2. 1 Dispersive enrichment

Radioactive elements are dispersively enriched in the cover rocks of Xiangshan volcanic basin. Among the cover rocks, porphyroclastic lava is highest in thickness and radioactive elements content mass fraction, average uranium and thorium contents being 8.65×10^{-6} and 26.48×10^{-6} respectively, not only much higher than the contents for adjacent metamorphic rocks as the basement of the basin (U: 3.31×10^{-6} , Th: 11.05×10^{-6} , ^{40}K : 1.90%; radioactive heat production (A): $1.85 \mu\text{W}/\text{m}^3$), but also exceeding the Clarke values of uranium and thorium for granite (U: 4.75×10^{-6} , Th: 1.85×10^{-6}). Assuming the average heat production and thickness for the cover rocks being $3.78 \mu\text{W}/\text{m}^3$ and 3 km separately, the radioactive heat flow will be $11.34 \text{ mW}/\text{m}^2$, while that for the normal granite will be $8.52 \text{ mW}/\text{m}^2$. Therefore, the heat flow produced by dispersive enrichment of radioactive elements is $2.82 \text{ mW}/\text{m}^2$, making up some 25% of the radiogenic heat flow and about 3.4% of the terrestrial heat flow for the study area. Considering the radioactive heat production for the basement rocks ($1.85 \mu\text{W}/\text{m}^3$), the dispersive enrichment of radioactive elements could produce $5.79 \text{ mW}/\text{m}^2$, contributing to about 7% of the terrestrial heat flow for Xiangshan Uranium Ore-field.

2. 2. 2. 2 Uranium deposits

In all deposits of Xiangshan Uranium Ore-field, uranium and thorium have been enriched at several orders of magnitude. Such radiogenic heat by concentric enrichment of U and Th makes up 0.6%~8.22% of total surface heat flow value, or higher.

2. 2. 3 The activity of ground water

In Jiangxi, the activity of groundwater is complex, and there are a lot of hot springs, which could affect the heat flow values. However, it is possible to correct the influences. The results of correction shows that the influence of movement of ground water on regional surface heat flow is quite obvious (see Table 1).

2. 2. 4 The topography

Most regions in Jiangxi Province belong to hilly land, but most of measured bore-holes distribute in the mountain area, variation of relief rather strong, and the depth of measured boreholes generally no exceeded 1000 m, so surface heat flow certainly accepts the effect of variation of relief. In order to eliminate these influence correcting calculation had been performed for part of holes. The results of cal-

ulation are shown in Table 1.

2.2.5 The magmation

obviously, the large scale of magmatic intrusion and eruption occurred in Jiangxi Province during the Yanshan Periods about 80 Ma ago can not affect the present heat flow.

The last magmatism in Jiangxi Province appeared in the Tertiary (about 9.4 Ma ago), but its scale is very small, and is mostly in the form of veins or dikes with areas less than 1 km². Therefore, their remained heat had already all lost, and it can not offer the obvious effect on terrestrial heat flow.

In summary, the effects on surface heat flow in Jiangxi Province are complicated. However, it is clear that the activity of ground water and topography are the key factors, the enrichment of radioactive elements and the activity of fault are the secondary factors.

3 GENERAL VIEWS OF THERMAL WATERS IN JIANGXI PROVINCE

Jiangxi Province is located within the active geothermal zone in the southeastern coastal area of China, and is also one of the provinces in which thermal waters are widely distributed. Ninety-six hot springs and more than 20 drill holes thermal waters have been found. Four typical hot spring areas, Maanping and Linchuan in the central Jiangxi, Lushan in the north, and hot springs in the south, will be discussed below.

3.1 Distribution

Thermal waters occur in rocks of different types and ages all over Jiangxi. They have a very close relations with geological structures. Most hot springs in Jiangxi are located along NE-trending and NNE-trending faults. Places which combined and crossed by NE-trending faults with NW-trending faults are the most favorable to the formation of hot springs (see Fig. 1).

Maanping Hot springs and Linchuan hot springs are the typical thermal waters in the central Jiangxi province. General geological setting of the Maanping hot-spring area can be seen from Fig. 2. Strata exposed in the area include Sinian system (Z) which is mainly composed of schist and phyllites, Cretaceous system (K) which consists of fluvial, proluvial and talus poists. In addition, granitites (γ_3^2) formed in Yanshanian can be found in the area. Geological structures in the area mainly a NE-trending great fault (F_1) and small NW-trending faults (F_2 , F_3).

Linchuan Hot springs occur along the same deep-great fault as Maanping hot springs do (see Fig. 2). It can be seen from Fig. 3 that the general geology in the Linchuan hot-springs area is similar to that in the Maanping hot spring area discussed above. Rocks exposed in the area are mainly phyllites and schists of Sinian system (Z), sandstones of Carboniferous system (C), sandstones and conglomerates of Cretaceous system (K) and sediments of quaternary system (Q). The sulfate and chloride contents of the rocks in the area are higher than those of the rocks in the Maanping hot spring area. In addition granites in yanshanian can be also seen in the area.

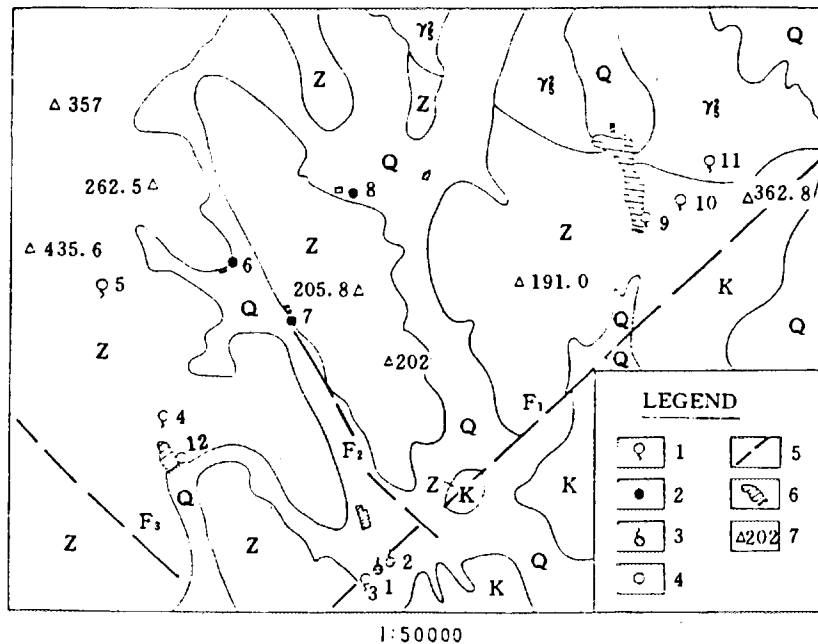


Fig. 2 Geological map and sampling location of Maanping hot spring area

1. cold springs; 2. well water; 3. hot springs; 4. surface water;
5. faults; 6. reservoir; 7. altitude (m).

The most important thermal water area in the northern Jizngxi province is the Lushan hot-spring area, which is located at the south western foothill of Mt. Lushan, 40 km south of Jiujiang City. General geological settings of the area are shown in Fig. 4. Strata exposed in the area include Precambrian system (Pt) which consists of Migmatitic granites, biotite gneiss and migmatized schists, Sinian system (Z) which is mainly composed of gneiss, quartz sandstones, tuff and conglomeratic sandstones, and Quaternary system (Q) sediments. Lushan hot springs are controlled by the NE-trending Ganjiang deep fault which is proved to be still active. Mt Lushan has been rising and its surrounding areas has been relatively sinking, the raised surface on the top of Mt. Lushan has been displaced by active faults, and more

than 10 earthquakes have taken place in the area for the past 500 years.

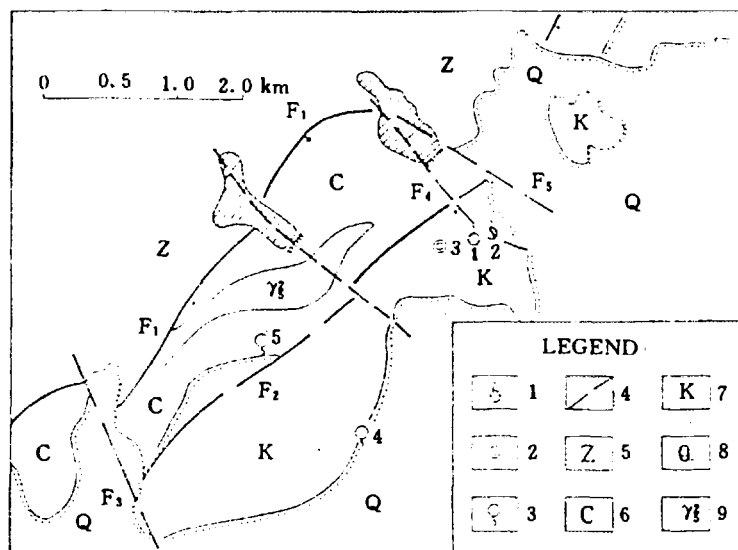


Fig. 3 Geological schematic map of Linchuan hot spring area

1. hot spring; 2. borehole; 3. cold springs; 4. fault; 5. Sinian system;
6. Carboniferous system; 7. Cretaceous system; 8. Qua ternary system; 9. Yanshanian granite.

3.2 Temperature

Thermal waters in Jiangxi have temperatures ranging from 23 °C to 88 °C at the outflow from drill holes or springs. Among them, more 80% are in the range of 20 °C to 60 °C (Table 2).

Table 2 Summary of water temperature of thermal water in Jiangxi province

Temperature/°C	20~40	40~60	60~80	>80
No. of thermal waters	66	36	13	3
Percentage/%	56	30.5	11	2.5

3.3 Rate of discharge

Up to date, researches reveal that the outflow of hot springs and drill hole thermal waters in Jiangxi Province is ranging from lower than 1 L/s to higher than 30 L/s. About 80% of them is in the range of 1 L/s to 3 L/s.

3.4 Sampling and analysis

Samples were taken from cold springs, wells, hot springs and surface water in the research areas, and the samples were collected in air tight glass bottles of 200 ml volume. Field parameters also measured for data supporting such as pH value, temperature and geological condition.

The chemical analyses were mainly conducted by chemical methods and partly on the 4500i type ion chromatography. The δD and $\delta^{18}O$ values were determined

by MAT251 mass spectrometer, and tritium contents in the water samples were determined using LSC-LBI type low background liquid scintillation counter.

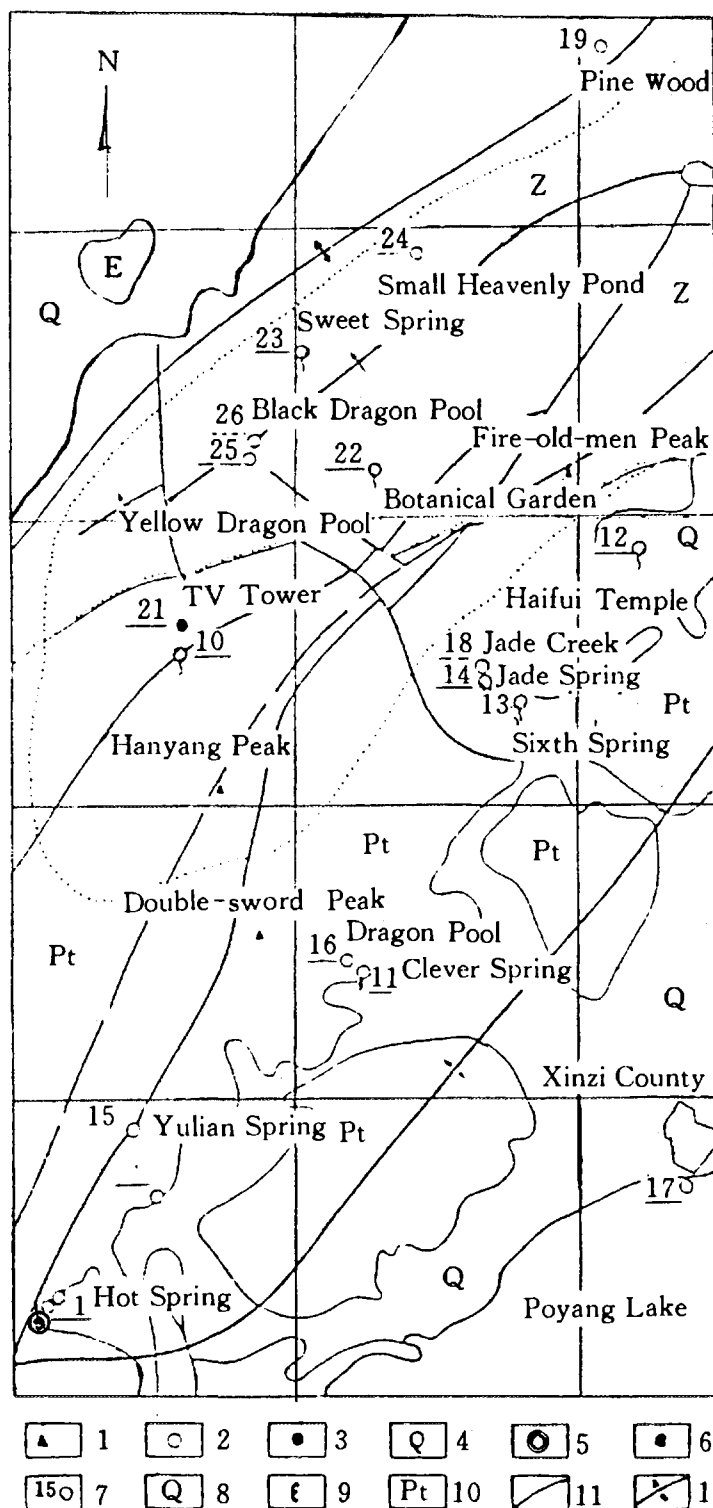


Fig. 4 Schematic map showing geological setting and sampling of Lushan hot-spring area

1. peak & altitude;
2. surface water;
3. well;
4. spring;
5. borehole;
6. thermal water;
7. No. of sampling;
8. Quarternary;
9. Cambrian;
10. Sinian;
11. fault;
12. anticlinal axis.

4 HYDROCHEMISTRY

The hydrochemical composition of the hot spring (MN2) in Maanping hot springs area in different years is given in Table 3, and the chemical analyses of other natural waters in the area are listed in Table 4.

Table 3 and Table 4 show that the hydrochemical types of cold ground waters in the area are HCO_3^- Na-Ca and HCO_3^- -Ca-Mg with very low TDS and weak-acid pH values. The types of waters are of typical hydrochemical characteristics in the humid climate area, southeastern China. The concentrations mass concentration of SiO_2 and other constituents, and TDS of thermal waters in the area are obviously higher than those of the local cold ground waters.

Table 3 Hydrochemical composition of Maanping hot-spring (MN2) in different year
(Concentration in 10^{-6})

Year	$\frac{T_w}{C}$	pH	$\frac{TDS}{g/L}$	HCO_3^-	SO_4^{2-}	Cl^-	NO_3^-	F^-	Ca^{++}	Mg^{++}	K^+	Na^+	SiO_2	Hydrochemical type
1985	43	6.1	1.41	940.8	42.0	10.98	0.30	7.0	117.3	11.9	120.7	167.8	60	HCO_3^- -Na-Ca
1987	41	61.9	1.23	835.7	30.0	8.88	0.82	3.13	96.4	9.9	97.5	147.5	50	HCO_3^- -Na-Ca
1992	41	6.4	1.20	837.6	28.0	8.93	0.83	3.6	102.9	8.7	92.0	120.0	50	HCO_3^- -Na-Ca

Note: T_w —water temperature; TDS—total dissolved solids.

Table 4 Hydrochemical composition of natural waters in Maanping hot-spring area
(Concentration in 10^{-6})

No.	Location	$\frac{T_w}{C}$	pH	$\frac{TDS}{g/L}$	HCO_3^-	SO_4^{2-}	Cl^-	Ca^{++}	Mg^{++}	K^+	Na^+	SiO_2	Hydrochemical type
1	MN1	42	6.13	1.24	835.7	30.0	9.23	109	4.88	97.5	145	60	HCO_3^- -Na-Ca
3	WB	20	5.97	0.021	10.98	1.4	0.25	1.5	0.61	2.5	2.0	25	HCO_3^- -Na-Ca
4	TB	18	5.8	0.031	23.5	0.15	0.2	4.0	2.1	0.3	0.2	16	HCO_3^- -Ca-Mg
5	XX	17.5	5.9	0.032	15.3	0.05	0.5	1.2	0.2	2.9	1.7	10	HCO_3^- -Na-Mg
6	DT	19	6.4	0.059	45.8	0.10	0.5	8.0	4.0	0.62	0.38	14	HCO_3^- -Na-Mg
7	XT	22	6.1	0.074	57.3	0.05	0.6	10.8	4.9	0.20	0.10	14	HCO_3^- -Na-Mg
8	SW	20	6.8	0.036	25.0	0.5	0.4	3.0	0.4	4.3	2.0	16	HCO_3^- -Na-Ca
10	CD	19	5.6	0.029	19.8	1.5	0.6	1.6	1.8	2.4	1.3	12	HCO_3^- -Na-Mg-Ca
11	ZL	20	6.5	0.037	26.2	1.0	0.6	2.3	1.8	3.1	2.0	20	HCO_3^- -Na-Mg-Ca

Hydrochemical composition of natural waters in the Linchuan hot-spring area is given in Table 5. It is clear that the waters in this area is of hydrochemical characteristics by leaching of local rocks. But the hydrochemical types of natural waters can vary from place to place mainly depending on the slight differences in lithochemistry, for thermal waters, HCO_3^- - SO_4^{2-} -Ca and HCO_3^- - SO_4^{2-} -Ca-Na are found, and for cold groundwaters, HCO_3^- - SO_4^{2-} -Cl-Ca-Na and HCO_3^- -Cl-Na-Ca are seen in the area. The thermal waters have low salinity, neutral-weak alkaline pH values and

high SiO₂ contents, while the cold ground waters have much lower salinity, neutral-weak acid pH values and lower SiO₂ contents.

Table 5 Hydrochemical composition of natural waters in Linchuan hot-spring area
(Concentration in 10⁻⁶)

No.	Location	$\frac{T_w}{C}$	pH	$\frac{TDS}{g/L}$	HCO ₃ ⁻	SO ₄ ⁻	Cl ⁻	Ca ⁺⁺	Mg ⁺⁺	K ⁺	Na ⁺	SiO ₂	Hydrochemical type
1	No. 1 Linchuan hot spring (LC1)	40.5	7.55	0.294	135.7	17.04	21.87	32.97	3.12	5.41	4.25	70	HCO ₃ -SO ₄ -Ca
2	No. 2 Linchuan hot springs (LC2)	38.5	7.4	0.221	121.06	33.62	6.68	48.10	4.87	3.87	2.91	60	HCO ₃ -SO ₄ -Ca
3	The ZK01 drill hole thermal water	59	8.27	0.358	130.84	72.00	2.49	61.12	2.19	15.5	13.5	80	HCO ₃ -SO ₄ -Ca-Na
4	Yueqian, cold spring (YQ)	19	6.99	0.0471	9.27	2.98	1.63	1.64	0.62	1.88	1.02	30	HCO ₃ -SO ₄ -Cl-Na-Ca
5	Tong-shanmiao cold spring (TM)	18	5.89	0.039	12.31	1.25	1.63	1.02	0.25	2.45	2.20	18	HCO ₃ -Cl-Na-Ca

According to the silica geothermometer, the temperatures of the geothermal reservoirs have been calculated to be from 106°C to 124°C, which indicates that the thermal waters belong to the low-medium temperature type geothermal resources.

The hydrochemical composition of natural water in the Lushan hot-spring area are also given in Table 6. It can be seen from Table 6 that the hydrochemical types of natural waters in the area are HCO₃-Na for thermal waters and are HCO₃-Na, HCO₃-Ca-Na-Mg, HCO₃-Ca, HCO₃-SO₄-Na-Ca and SO₄-Ca for cold ground waters. The thermal water is characterized by low salinity, alkaline deep circulation leaching water, while cold ground waters are of very low salinity, weak acidic to neutral leaching characteristics. The silica and fluorine contents of the thermal water are much higher than those of the local cold ground waters, which mainly depends up on the circulation distance and water temperature.

By means of the silica geothermometer, the temperature of the geothermal reservoir for the Lushan hot spring is estimated to be about 125°C. The maximum circulation depth of the thermal water is 4000 m or so for the geothermal gradient in the area is about 29°C/1000 m.

In summary, thermal waters in Jiangxi are generally characterized by low salinity (0.3~0.5 g/L), moderate to high pH values (most are larger than 7.5), high HCO₃-Na and HCO₃-Na-Ca, HCO₃-SO₄-HCO₃-Na. Other hydrochemical types such as HCO₃-CO₃-Na, CO₃-HCO₃-Na and HSiO₃-Na can be also found in the province

Table 6 Isotopic and hydrochemical composition of natural waters in the Lushan hot-spring area
(Ion concentration in 10^{-6})

Sample	T_w °C	pH	TDS g/L	HCO ₃ ⁻	SO ₄ ²⁻	Cl ⁻	F	K ⁺ +Na ⁺	Ca ²⁺	Mg ²⁺	SiO ₂	δD ‰	$\delta^{18}O$ ‰	δ^2H T. U.	Sampling altitude m	Hydrochemical type
CK-1, Hot water (drill hole)	71	8.60	0.424	185.56	14.4	5.50	15.0	110.1	1.72	0.0	80.0	-52.9	-8.06	<1	40	HCO ₃ -Na
SI-2, Lushan hot spring	65	8.78	0.385	173.85	13.0	5.14	15.0	96.0	2.71	0.69	90	-49.6	-7.98	<1	40	HCO ₃ -Na
CK-6, Cold water (drill hole)	19	7.34	0.145	71.13	0.0	0.64	—	9.0	10.14	4.2	50	-38.8	-6.37	36.6	40	HCO ₃ -Ca-Na-Mg
L-10, Guizong temple well	20	6.60	0.267	103.33	20.0	23.08	—	23.5	37.49	4.99	45	-36.1	-6.24	15.5	60	HCO ₃ -Cl-Na-Mg
L-11, Clever spring	19	5.90	0.084	27.09	3.5	3.83	0.1	10.1	4.15	0.0	33	-34.6	-6.82	<1	60	HCO ₃ -Cl-Na-Ca
L-12, Hailui temple spring	23	6.65	0.025	8.12	2.8	0.781	0.8	3.3	1.10	0.097	8	-42.6	-7.20	20.3	330	HCO ₃ -SO ₄ -Na-Ca
L-13, The sixth spring	19	6.17	0.032	8.12	2.8	0.781	0.0	3.5	0.73	0.243	16	-42.8	-7.07	12.7	130	HCO ₃ -SO ₄ -Na-Ca
L-14, Jade creek spring	19	5.80	0.045	15.99	0.0	0.639	0.0	5.5	0.62	0.097	21	-43.6	-7.24	23.4	145	HCO ₃ -Ca-Na-Mg
L-15, Yulian spring	19	6.79	0.025	8.12	2.6	0.639	0.0	3.0	1.26	0.097	9	-38.7	-6.94	—	240	HCO ₃ -SO ₄ -Na-Ca
L-16, Dragon pool	19	7.26	0.055	29.28	3.0	1.67	0.0	3.5	7.11	1.155	8.8	-40.5	-6.56	—	70	HCO ₃ -Ca-Na-Mg
L-17, Poyang lake	21	7.26	0.050	28.30	0.0	1.28	0.0	2.5	6.95	1.05	8.8	-35.2	-5.85	17.4	20	HCO ₃ -Ca
L-18, Jade creek stream	20	7.38	0.032	13.55	2.6	1.03	0.0	3.3	2.37	0.474	8.8	-41.2	-7.38	—	140	HCO ₃ -SO ₄ -Na-Ca
L-19, Pine wood spring	18	6.75	0.020	2.93	4.0	0.64	0.0	2.0	1.64	0.19	6	-42.9	-7.36	21.6	541	SO ₄ -Na-Ca
L-20, TV tower	17	6.51	—	—	—	—	—	—	—	—	—	-45.2	-7.71	12.2	1304	—
L-21, TV well	18	—	—	—	—	—	—	—	—	—	—	-44.9	-7.96	17.1	1320	—
L-22, Botanical garden	18	—	—	—	—	—	—	—	—	—	—	-48.1	-7.88	28.0	1111	—
L-23, Sweet spring	19	—	—	—	—	—	—	—	—	—	—	-46.6	-7.66	33.0	980	—
L-24, Small heavenly pond	18	—	—	—	—	—	—	—	—	—	—	-41.6	-7.44	—	1210	—
L-25, Lushan sanatorium	20	—	—	—	—	—	—	—	—	—	—	-43.2	-7.68	—	—	—
L-26, Black dragon pool	19	—	—	—	—	—	—	—	—	—	—	-43.2	-7.43	—	870	—

5 ISOTOPES

5.1 $\delta^{18}\text{O}$, δD and interpretation

5.1.1 Origin of thermal water

Stable oxygen and hydrogen isotopic composition for the natural waters in Lushan, Maanping, Linchuan and southern Jiangxi have been listed in Table 6, 7, 8 and 9.

Table 7 Isotopic composition of natural waters in Maanping area

No.	Samples	Temperature/°C	$\delta\text{D}/\text{‰}$	$\delta^{18}\text{O}/\text{‰}$
1	No. 1 hot spring (MN1)	41.5	-44.1	-7.23
2	No. 2 hot spring (MN2)	41.0	-45.4	-6.84
3	WB (cold spring)	20.0	-34.3	-5.46
4	TB (cold spring)	18.0	-36.9	-5.70
5	XX (cold spring)	17.5	-37.4	-5.93
6	DT (cold spring)	19.0	-29.8	-5.15
7	XT (well)	22.0	-35.4	-5.60
8	SW (well)	20.0	-42.3	-6.30
9	CJ (cold spring)	21.0	-22.3	-3.97
10	CD (cold spring)	19.0	-35.8	-5.57
11	ZL (cold spring)	20.0	-35.6	-5.78
12	WX (water reservoir)	20.0	-31.8	-4.43

Cold springs and well water in Maanping are all shallow groundwater whose isotopic composition can reflect the mean isotopic value of meteoric water in the area (Table 7). According to the isotopic data of these shallow cold groundwater samples (XX, XT, DT, SW, CD, ZL, TB, WB, CJ), the local meteoric water line in the Maanping hot-spring area can be obtained (correlation coefficient r is 0.98) as follows:

$$\delta\text{D} = 8.4 \delta^{18}\text{O} + 11.8 \quad (2)$$

The local meteoric water line is similar to the global meteoric water line obtained by Craig (1961) ($\delta\text{D} = 8 \delta^{18}\text{O} + 10$). The $\delta^{18}\text{O}$ and δD values of Maanping hot springs are roughly in line with the local meteoric water line (Fig. 5), which indicate that the thermal water are of meteoric origin. It is also seen from Fig. 4 that no obvious oxygen shift has been found. The evidence reveals that the temperatures of the deep geothermal reservoirs are not high and the thermal waters belong to the deep circulation type and low enthalpy geothermal resources. In addition, according to the silica geothermometer (R. O. Fournier, 1981), the temperatures of the geothermal reservoirs have been calculated to be from 102 to 110°C, which is in accord with the above-mentioned inference.

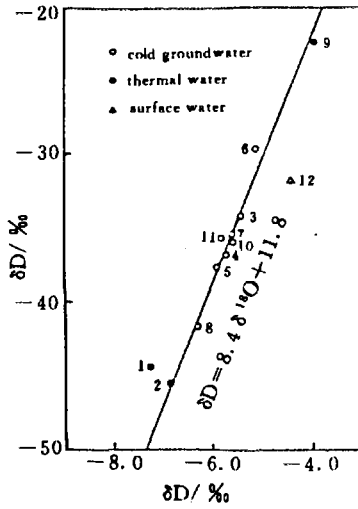


Fig. 5 The δD - $\delta^{18}O$ plot for natural waters Maanping hot-spring area

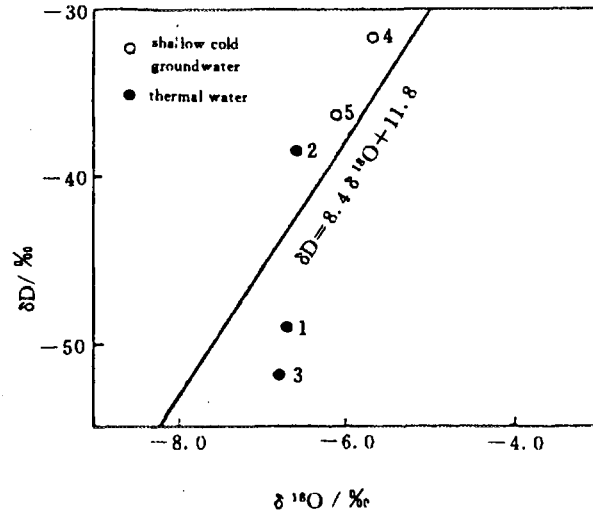


Fig. 6 The δD - $\delta^{18}O$ plot for natural waters in Linchuan hot-spring area

Table 8 Isotopic composition of natural waters in Linchuan hot-spring area

No.	Location	T_w	δD ‰	$\delta^{18}O$ ‰	$\frac{^3H}{T.U}$	Sampling Altitude	Recharge by $\delta^{18}O$	Altitude by δD
						m		m
1	LC1	41.5	-49.0	-6.70	0.33	62.1	569.7	690.3
2	LC2	38.5	-38.4	-6.57		62.0	530.3	348.4
3	ZK01	59.0	-52.0	-6.80		63.0	600.0	787.1
4	YQ	19.0	-31.7	-5.66		71.4		
5	TM	18.0	-36.2	-6.13		220		

The climatic and topographic conditions for Linchuan hot-spring area are just the same as those in the Maanping hot-spring area, so the local meteoric water line in the Maanping hot-springs area is used here (Fig. 6). It can be seen that all the data points for thermal water samples in Linchuan hot-spring area fall in proximity to the local meteoric water line, which indicates that the thermal water are of the same origin as the meteoric water.

Table 8 and Fig. 6 also show clearly that the isotopic composition of the No. 1 sample is similar to that of the No. 3 sample, but different from that of the No. 2 sample. The evidence may imply that the thermal waters come from two different aquifers. In addition, the different in silica content of the thermal water also suggests such possibility. Fortunately, the inference has recently been proved by the ZK02 drill hole which locates about 200 m west of the ZK01 drill hole (Ling, Q., 1992). The ZK02 drill hole reveals that there exist two thermal water aquifers in the area, the first lies from 73.5 to 121.10 m below the ground, the second lies

from 156.6 to 272.32 m under the ground.

The δD and $\delta^{18}O$ composition for natural waters in Lushan hot-spring area have been shown in Table 6. By regressive analysis of these samples, a linear equation has been obtained as follows:

$$\delta D = 7.16 \delta^{18}O + 8.88 \quad (\gamma = 0.98) \quad (3)$$

Which is taken as the local meteoric water line for Lushan hot-spring area. The $\delta^{18}O$ and δD values of Lushan thermal waters are roughly in accord with the local meteoric water line (Fig. 7) which reveals that thermal waters are of local meteoric origin. According to the calculation by the silica geothermometer, the temperature of the geothermal reservoir is about 124°C, which indicates the thermal water in the area belongs to low-medium temperature category.

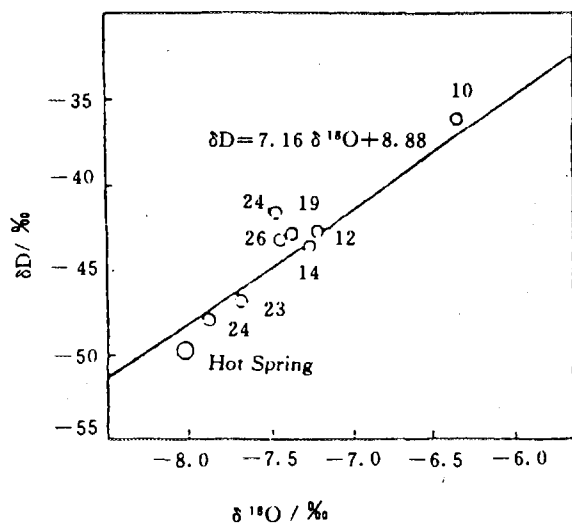


Fig. 7 The δD and $\delta^{18}O$ compositions of natural waters in Lushan area

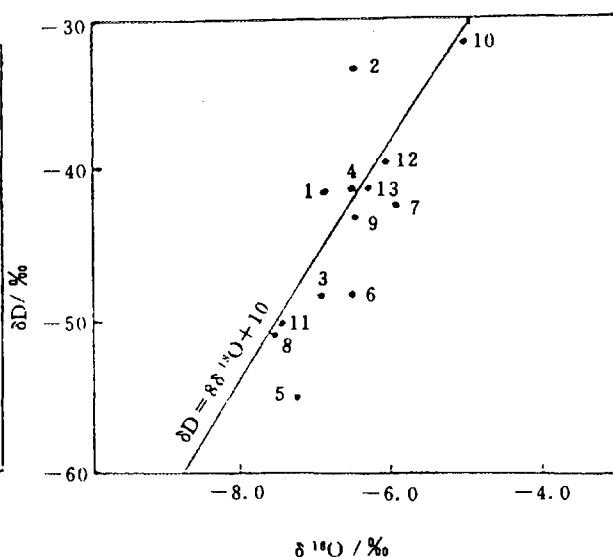


Fig. 8 The δD - $\delta^{18}O$ plot for natural waters in the southern Jiangxi province

The southern part of Jiangxi province is mountainous and rich in mineral resources geothermal waters. In the region, a lot of thermal springs have been found (see Figure 1) and many isotopic samples of natural waters have been taken for the past two years. Some of the samples have been analyzed (the results are given in Table 9).

It can be seen from Table 9 and Fig. 8 that the isotopic composition of natural waters in the area are basically in line with the Craig Line. Evidently, the thermal water and other natural waters are of local meteoric origin. However, owing to the limitation of time and funds, the intensive isotopic hydrogeological studies and the

comprehensive evaluation of the geothermal resources in the southern Jiangxi need to be made in the future.

5.1.2 The altitude calculation of the recharge area of thermal water

It is well known, in a given region, the δ -values of precipitation at higher altitudes generally will be more negative. In order to determine the altitude effect of precipitation in Maanping hot-spring area, some shallow cold groundwater samples whose recharge areas are clear have been collected and regarded as the mean precipitation at corresponding altitudes (see Table 10).

Table 9 Isotopic composition of some natural waters in southern Jiangxi province

No.	Sample and location	$\delta D/\text{‰}$	$\delta^{18}\text{O}/\text{‰}$
1	No. 1 Mine water, Piaotang	-41.28	-6.89
2	No. 2 Mine water, Piaotang	-33.18	-6.54
3	No. 3 Mine water, Piaotang	-48.42	-6.94
4	No. 1 Mine water, Tongping	-41.30	-6.52
5	No. 1 Mine water, Tongping	-55.35	-7.25
6	No. 1 Mine water, Xihuashan	-48.37	-6.52
7	No. 2 Mine water, Xihuashan	-42.28	-5.94
8	No. 3 Mine water, Xihuashan	-50.74	-7.60
9	No. 4 Mine water, Xihuashan	-43.00	-6.50
10	No. 1 Cold Spring, Xihuashan	-31.14	-5.14
11	No. 1 Mine water, Wunwu	-50.10	-7.50
12	No. 1 Xunwu hot spring	-39.02	-6.09
13	Mine water, Baoshan	-40.60	-6.34

Table 10 Isotopic composition and recharge altitude of cold springs in Maanping hot-spring area

No.	Samples	$\delta^{18}\text{O}/\text{‰}$	$\delta D/\text{‰}$	Recharge altitude/m
4	TB	-5.70	-36.9	250
5	XX	-5.93	-37.4	350
6	DT	-5.15	-29.8	110
7	CD	-5.57	-35.8	220
8	ZL	-5.78	-35.6	280

According to the data listed above, the altitude-isotopic composition correlation lines of the mean precipitation can be obtained as follows:

$$\delta D = -27.6 - 0.031h \quad (\gamma = -9.90) \quad (4)$$

$$\delta^{18}\text{O} = -4.82 - 0.0033h \quad (\gamma = -9.99) \quad (5)$$

where, $\delta^{18}\text{O}$ values are expressed in $\delta(\text{‰})$ versus SMOW; h means altitude (meters) and γ is correlation coefficient.

It is clear that the altitude gradients in the area are $0.33\text{‰}/100\text{ m}$ for $\delta^{18}\text{O}$ and $3.1\text{‰}/100\text{ m}$ for δD . The values are in the range of typical gradients in $\delta^{18}\text{O}$

of between $0.15\text{‰}/100\text{ m}$ and $0.5 \times \text{‰}/100\text{ m}$ and gradients in δD of between about $1.5 \times \text{‰}/100\text{ m}$ and $4 \times \text{‰}/100\text{ m}$ (Gat & Gonfiantini, 1981). Based on the Eqs. (4) and (5), the altitudes of recharge area for Maanping hot-spring have been calculated and are given in Table 11. The recharge altitudes are approximately ranging from 500 to 800 m, which is close to the altitude obtained by traditional hydrogeological analysis.

Furthermore, according to isotope altitude effect rule and the result of the Maanping hot-springs area discussed above, the altitude of the recharge area for Linchuan thermal waters is estimated to be about from 300 m to 700 m higher than that of the discharge area where the thermal waters occur (see Table 11). The result is roughly in accord with that obtained by traditional hydrogeochemical methods (Zhang, W. M., 1990).

Table 11 Recharge altitude of thermal water calculated by δD and $\delta^{18}O$ in Maanping hot spring area

No.	Location	$\frac{\delta D}{\text{‰}}$	$\frac{\delta^{18}O}{\text{‰}}$	Discharge altitude (sampling altitude) m	Recharge altitude (by $\delta^{18}O$), (by δD)	
1	MN1	-44.1	-7.23	87	730.3	532
2	MN2	-45.4	-6.84	86	612.1	574

In order to determine the altitude effect of precipitation in the Lushan hot spring area, some shallow cold ground water samples whose recharge areas are known have been taken and regarded as the mean precipitation at corresponding altitudes (see Table 12), and the altitude isotopic composition correlation lines are as follows:

$$\delta D = -0.0138h - 35.34 \quad (\gamma = -0.609) \quad (6)$$

$$\delta^{18}O = -0.0018h - 6.33 \quad (\gamma = -0.716) \quad (7)$$

Where, the δD and $\delta^{18}O$ values are expressed in $\delta(\text{‰})$ versus SMOW; h means altitude (meters), and γ is correlation coefficient.

The altitude of the Lushan hot springs recharge area is estimated to be about 1100 m by Eq. (7) and about 1050 m by Eq. (8) respectively. In fact, the planation surface of Mt. Lushan is ranging from 850 m to 1100 m above sea level. Geological, hydrogeological and physiographical analyses show that the recharge area of Lushan hot springs should be above the planation surface which is an ancient eroded basin of 75 km². In the area, the annual precipitation rate is about 1833 mm, and the fractures and weathering crevices serve as good paths for infiltration of local meteoric water.

5.2 Radioactive isotopes

5.2.1 Tritium and thermal water dating

The tritium content of shallow cold ground waters determined for Maanping hot spring area is given in Table 12. Roughly, it reflects the annual mean tritium content of local precipitation. The tritium values of hot springs in the area in different time are listed in Table 13.

Table 12 Tritium content of shallow cold ground water in Maanping hot-spring area

No.	7	8	11	3
(location)	(XT)	(SW)	(ZL)	(WB)
Type of water	well	well	cold spring	cold spring
Tritium/T. U	39.7	32.9	43.6	33.3

Table 13 Tritium content of Maanping hot-spring in different time

No.	Samples	Date	Tritium/T. U.
1	MN1	May, 1985	<1
		May, 1987	10.0
2	MN2	May, 1985	1.9
		May, 1987	7.5

It can be seen from Table 13 that the tritium content of Maanping hot spring in area increased from 1985 to 1987. In order to find the cause of the change, hydro-geological survey in the area has been made and revealed that is due to the mixing of thermal water and shallow cold ground waters. The mixing will be discussed later. Probably the tritium content measured in 1985 is the true value of pure thermal water (non-mixed water), which indicates that the thermal water was recharged by meteoric water before the beginning of thermonuclear tests.

Table 14 Radium and radon content of Maanping hot springs

No.	Location	Rn/Bq · L ⁻¹	Ra/Bq · L ⁻¹	N _{Ra} /N _{Rn}	Age/a
1	MN1	20.4	0.685	0.0336	79
2	MN2	26.0	0.892	0.0342	80

In addition, radium and radon concentrations of hot springs in the area have been measured and are given in Table 14. According to the dating equation by Cherdyntsev (1969):

$$t = -1/\lambda \times \ln(1 - N_{Ra}/N_{Rn}) \quad (8)$$

where, t is the age of water (years); λ is the decay constant of radium (4.33×10^{-4}); N_{Ra} and N_{Rn} are the radium and radon of water respectively.

The estimated age of the thermal water in Maanping hot-spring area is about 80 a, which supports the above-mentioned conclusion. Furthermore, the hydro-chemical type of the thermal water is brackish HCO₃-Na-Ca (Table 3 and Table

4) which is typical for the low-moderate temperature thermal water formed by the deep circulation of meteoric water for decades under ground.

According to the tritium content of the hot spring (LC1), the thermal water is estimated to be recharged by meteoric water before the beginning of thermonuclear tests. In addition, the radium and radon concentration of the hot spring (LC1) are 2.553 Bq/L and 52.15 Bq/L respectively. The age of the thermal water has been calculated to be about 116a by Cherdyntsev (1969) method. Obviously, the two results basically answers to each other.

In Lushan area, the tritium content of shallow groundwater and surface water is at least higher than 12 T. U., but that of thermal water is less than 1 T. U.. Obviously, the geothermal water has not been mixed with shallow cold groundwater or surface water and is older than 40 a. The radium and radon concentrations of Lushan hot spring are determined as 7×10^{-12} g/L and 5.11 Bq/L respectively, and the estimated age of the spring is about 80 a by the Cherdyntsev Method.

5.2.2 Identification of the mixing proportions of thermal waters and shallow cold ground water

From 1985 to 1987, a lot of rocks in Maanping hot-spring area have been extracted for building by local farmers. For the reason, infiltration of surface water and meteoric water have been increased, and the mixing between thermal waters and shallow cold groundwaters has also been increased. So the concentrations of constituents in thermal waters as the hot spring (MN2) (see Table 3) in the area has been diluted. In addition, the tritium content of thermal waters also demonstrate the change (see Table 13).

The mixing proportion of thermal waters and shallow cold groundwaters can be calculated by isotopic and hydrochemical methods. As it well known, in the course of movement from the depth to the top of geothermal reservoirs, thermal waters will mix with shallow cold groundwaters in different proportions. Their isotopic and hydrochemical compositions will take place some changes as a result of the mixture. In one hand, the salinity and ion concentrations of thermal waters are usually higher than those of shallow cold groundwaters. In other hand, their $\delta^{18}\text{O}$, δD and ^3H values are commonly lower than those of shallow cold groundwaters because thermal waters have longer circulation distance and larger altitude of the recharge areas.

In order to determine the proportions of water of different genesis in a reservoir under study, the following mixing equation is in common use (taking tritium

for an example)

$$\begin{aligned} X + Y &= 1 \\ T_h \cdot X + T_c \cdot Y &= T_m \cdot (X + Y) \end{aligned} \quad (9)$$

where,

- X ——the proportion of thermal water, %;
- Y ——the proportion of shallow cold ground water, %;
- T_h ——the tritium content of thermal water, T. U.;
- T_c ——the tritium content of shallow cold ground water, T. U.;
- T_m ——the tritium content of mixed water, T. U.

The mixing proportions of hot water and shallow cold groundwater (recent infiltration water) for the hot spring (MN2) in the Maanping hot springs area has been estimated by Eq. (9). The relevant data are given in Table 12 and Table 13.

The tritium value of the hot spring (MN2) in 1985 was 1.9 T. U. (i. e. T_h in the equation), while the value in 1987 changed up to 7.5 T. U. (i. e. T_m in the equation) for mixing increase. The mean tritium content of shallow cold ground waters in the area was 38 T. U. (i. e. T_c in the equation) so we got that the shallow cold ground water occupied about 16% in the thermal water.

As above-mentioned, the TDS, Cl⁻ and other ion concentrations, and temperature of hot spring decreased from 1985 to 1987. Obviously the changes also showed the mixing between shallow cold ground water and hot water. According to the TDS of the hot spring before and after mixed, and the TDS of shallow cold ground waters nearby (their mean TDS is about 40 mg/L), we got that about 13% of the hot spring water (mixed water) is shallow cold ground water by the similar method as above. The percentage of shallow cold ground water basically answers to the abovementioned result.

During the 1987~1992, the hydrochemical composition of the thermal water from Maanping hot springs keep basically stable owing to the local extraction rock activities have been stopped and infiltration condition have not any distinct change.

6 CONCLUSIONS

(1) The average value of 20 measured terrestrial heat flow is (69.79 ± 13.40) mW/m². Separated by Zhe-Gan railway, the average value of measured heat flow in the north part of Jiangxi is (58.18 ± 3.75) mW/m², and the average value of 15 measured terrestrial heat flow in the central-south part is (74.10 ± 13.6) mW/m². The general distribution rule of measured heat flow is lower in the

north and higher in the central-south parts.

(2) Along the deep-great faults, the transitional zone of deep structure and in the uranium-riched area or uranium deposits, the heat flow is obviously increased, even becoming anomalies. The distribution of anomalies of heat flow is coincident with the area of thermal water and volcanic and magmatic activity in Mesozoic and Cainozoic. All of them are controlled by deep-great faults and the transitional zone of deep structure.

(3) The thermal waters in Jiangxi province are of meteoric origin and are formed by the deep circulation of local meteoric water along the deep fault.

(4) The hydrochemical compositions of the thermal waters are mainly characterized by low salinity $\text{HCO}_3\text{-Na}$, $\text{HCO}_3\text{-Na-Ca}$ and $\text{HCO}_3\text{-SO}_4\text{-Ca-Na}$ types.

(5) The thermal waters were recharged before the beginning of thermonuclear tests.

(6) The altitude gradients in northern Jiangxi province are 0.18/100 m for $\delta^{18}\text{O}$ and 1.4/100 m for δD , while those in central Jiangxi are 0.33/100 m for $\delta^{18}\text{O}$ and 3.1/100 m for δD .

(7) The geothermal resources belong to the low-mid temperature category for the maximum water temperature of thermal springs at outflow points is less than 90°C and the geothermal reservoir temperature is about $100\sim 130^\circ\text{C}$.

In conclusion, the thermal energy of thermal waters in Jiangxi province is suitable for direct uses but not economic for power generation.

ACKNOWLEDGEMENTS

This research was supported by the China National Fund of Natural Sciences and the IAEA Research Contract No. 6447/R0/RB and No. 6447/RB. Thanks are extended to the staff members of the Lushan hot spring Sanatorium and the Linchuan hot spring Sanatorium in Jiangxi province.

REFERENCES

- 1 Cherdyntsev V V. Uranium-234. Moskva: Atomizdat, 1969
- 2 Craig H. Standard for Reporting Concentrations of Deuterium and Oxygen-18 in Natural Water. Science, 1961(133); 1833~1834.
- 3 Craig H. Isotopic Variation in Meteoric Waters. Science, 1961(133); 1702~1703
- 4 Dansgard W. Stabke Isotopes in Precipitation. Tellus 1964(16); 436~468
- 5 Ferronsky V I, Polyakov V A. Environmental Isotopes in the Hydrosphere. John Wiley & Sons, 1982

- 6 Fournier R. Application of Water Chemistry to Geothermal Exploration and Reservoir engineering. Geothermal Systems, Principles, Case Histories Reservoir Engineering. Rybach L, Muffler L J P. (eds), 1981, 109~140
- 7 Gat J R, Gonfiantini R. Stable Isotope Hydrology. IAEA, 1981
- 8 Li Xueli. The Relationship between Distribution of Thermal Waters and Uranium Mineralization in Jiangxi. Fuzhou; Journal of East China Geological Institute of , 1979(2); 21~29
- 9 LI Xueli. On the Mineralization Model of "Three Sources—Heat, Water and Uranium". Journal of East China Geological Institute, 1992(15); 101~112
- 10 LI Xueli. Study on the Relationship between Jiangxi Hot Springs Genesis and Uranium Mineralization. Journal of East China Geological Institute, 1992(15); 201~220
- 11 LI Xueli. Analysis on the geological Structure Conditions of Hot Springs in Jiangxi Province. Journal of East China Geological Institute, 1992 (15); 221~228
- 12 LI Xueli, ZHOU Wenbin, ZHANG Weimin, et al. Relations between Terrestrial Heat Flow and Uranium Deposits in Jiangxi Province, China. Water Rock Interaction. Kharaka & Maest, (eds). Balkema, Rotterdam, 1992, 1597~1599
- 13 SUN, Zhanxue. The Hydrogeochemical Characteristics and Origin of Thermal Water in Jiangxi, Southeast China. Water Rock Interaction. Miles, ed. Balkema, Rotterdam, 1989; 661~664

(京) 新登字 077 号

图书在版编目 (CIP) 数据

中国核科技报告 CNIC-01104 GIEC-0002: 江西省地
热背景与地下热水同位素地球化学研究: 英文/周文斌著.
—北京: 原子能出版社, 1996. 10

ISBN 7-5022-1574-3

I. 中… I. 周… III. 核技术-研究报告-中国-英文 IV.
TL-2

中国版本图书馆 CIP 数据核字 (96) 第 16198 号

江西省地热背景与地下热水同位素地球化学研究

周文斌等著

©原子能出版社, 1996

原子能出版社出版发行

责任编辑: 郭向阳

社址: 北京市海淀区阜成路 43 号 邮政编码: 100037

中国核科技报告编辑部排版

核科学技术情报研究所印刷

开本 787×1092 1/16·印张 1·字数 37 千字

1996 年 10 月北京第一版·1996 年 10 月北京第一次印刷

CHINA NUCLEAR SCIENCE & TECHNOLOGY REPORT

This report is subject to copyright. All rights are reserved. Submission of a report for publication implies the transfer of the exclusive publication right from the author(s) to the publisher. No part of this publication, except abstract, may be reproduced, stored in data banks or transmitted in any form or by any means, electronic, mechanical, photocopying, recording or otherwise, without the prior written permission of the publisher, China Nuclear Information Centre, and/or Atomic Energy Press. Violations fall under the prosecution act of the Copyright Law of China. The China Nuclear Information Centre and Atomic Energy Press do not accept any responsibility for loss or damage arising from the use of information contained in any of its reports or in any communication about its test or investigations.

ISBN 7-5022-1574-3



9 787502 215743 >